Journal of Environmental Chemical Engineering 11 (2023) 109823

Contents lists available at ScienceDirect

Journal of Environmental Chemical Engineering

journal homepage: www.elsevier.com/locate/jece

Chemical recycling of monolayer PET tray waste by alkaline hydrolysis

Asier Barredo [a,c,*], Asier Asueta [b,**], Izotz Amundarain [b], Jon Leivar [b], Rafael Miguel-Fernández [b], Sixto Arnaiz [b], Eva Epelde [c], Rubén López-Fonseca [c], José Ignacio Gutiérrez-Ortiz [c]

[a] Department of Chemical and Environmental Engineering, Faculty of Engineering Bilbao, University of the Basque Country (UPV/EHU), Plaza Ingeniero Torres Quevedo 1, E-48013 Bilbao, Spain
[b] GAIKER Technology Centre, Basque Research and Technology Alliance (BRTA), Parque Tecnológico de Bizkaia, Edificio 202, E-48170 Zamudio, Spain
[c] Department of Chemical Engineering, University of the Basque Country (UPV/EHU), Barrio Sarriena s/n, E-48940 Leioa, Spain

ARTICLE INFO

Editor: Chao He

Keywords:
Polyethylene terephthalate waste
Chemical recycling
Alkaline hydrolysis
Phase transfer catalyst
Terephthalic acid
Kinetic modeling

ABSTRACT

The high demand for recycled polyethylene terephthalate (rPET) driven by an increase in environmental awareness, the application of more restrictive environmental legislations, together with the large increase in the generation of post-consumer PET plastic waste, has resulted in an urgent need for efficient recycling processes. In this work, alkaline hydrolysis is presented as a promising chemical recycling alternative for PET tray waste. PET depolymerization reactions were carried out under mild conditions (80–100 ºC and atmospheric pressure) using tributylhexadecylphosphonium bromide quaternary salt (TBHDPB) as catalyst. Several operating variables were studied based on PET conversion and terephthalic acid (TPA) yield criteria: (i) catalyst mass ratio of TBHDPB to PET (0–0.2); (ii) particle size (0.5–10 mm); (iii) stirring rate (350–700 rpm); and, (iv) temperature (80–100 °C). A good compromise between PET conversion (99.9%) and TPA yield (93.5%) was established after 4 h of reaction, under the following operating conditions: TBHDPB:PET catalyst ratio, 0.2; 100 °C; particle size, 1–1.4 mm; and, stirring rate, 525 rpm. In addition, the experimental kinetic data correctly fits to the proposed shrinking core model. Activation energy values of 60 and 57.4 kJ mol^{-1} were established for the non-catalyzed and catalyzed reactions, respectively, which implies that TBHDPB catalyst does not apparently modify the reaction mechanism.

1. Introduction

Polyethylene terephthalate (PET) is a linear thermoplastic polymer widely used in textiles and food packaging, given its good properties such as chemical and thermal resistance, low permeability towards CO_2 and lightness among others [1,2]. The current PET plastic waste management relies heavily on incineration and landfill, which are typical applied technologies in a linear polymer economy. This situation is driven by the huge demand for PET plastic products, together with its low recycling rate, which accounts for 23% in the European Union (EU) [2,3].

Within this scenario, the updated European Commission's PET recycling strategy calls for a mandatory 25% recycled PET content in PET beverage bottles by 2025, increasing to 30% by 2030 (currently 17%) [4]. This point is also reinforced by the European landfill tax, with a value of 0.80 €/kg for plastics deposited on landfill. From a business perspective, this trend is reinforced by the proliferation of voluntary agreements by large companies such as PepsiCo or Nestlé , which propose a greater use of recycled plastic material in their packaging [5,6]. These measures and trends have increased the demand for recycled PET, causing the price of rPET to exceed that of virgin PET [5,7]. For this reason, the development of efficient PET recycling technologies is necessary [8].

PET can be recycled or recovered through four pathways, namely primary recycling (on-site recycling of pure scraps), secondary recycling (mechanical recycling), tertiary recycling (chemical recycling), and quaternary recycling (incineration) [9–11]. Solvolysis is the chemical recycling technology applied for the depolymerization of condensation polymers such as PET [3,12]. Depending on the solvent used for degradation, solvolysis methods can be classified as glycolysis [13,14], hydrolysis [15,16], ammonolysis, aminolysis [17,18], and methanolysis [19,20]. Glycolysis is the most developed and industrially established

* Corresponding author at: Department of Chemical and Environmental Engineering, Faculty of Engineering Bilbao, University of the Basque Country (UPV/EHU), Plaza Ingeniero Torres Quevedo 1, E-48013 Bilbao, Spain.
** Corresponding author.
E-mail addresses: asier.barredo@ehu.eus (A. Barredo), asueta@gaiker.es (A. Asueta).

https://doi.org/10.1016/j.jece.2023.109823
Received 26 December 2022; Received in revised form 22 February 2023; Accepted 28 March 2023
Available online 31 March 2023

depolymerization process, which uses a glycol, most commonly ethylene glycol, as a degradation agent. Leading companies such as DuPont, Goodyear, Eastman, Kodak, Shell Polyester or Zimmer AG use glycolysis for the post-consumer recycling of PET [21]. In the case of methanolysis process, few technologies are making progress beyond laboratory stage [22]. For example, Loop Industries is already operating at pilot plant scale [23]. Regarding aminolysis and ammonolysis, even though there are demonstrations of lab-scale depolymerization, to date there is no evidence of a further implementation beyond this scale [24]. Other novel chemical recycling technologies, such as PET hydrolyzing enzymes, are still in early stages of development [25].

Hydrolysis is an alternative depolymerization method that allows operating under moderate conditions and also with highly contaminated post-consumer waste feeds [26]. PET hydrolysis can be classified as neutral [27], acid [16] and alkaline [3,28].

In neutral hydrolysis, water or steam is used in the presence of a transesterification catalyst (e.g. alkali metal acetate). Low purity terephthalic acid (TPA) is obtained, since impurities (i.e. metal catalyst, dyes, pigments, other glycols, and dicarboxylic acids) are not easily separated during the hydrolysis process [29]. In acid hydrolysis, large amounts of acids (>87 wt%), such as H_2SO_4, HNO_3 or H_3PO_4, are used [20], giving way to substantial amounts of inorganic and aqueous waste disposal, together with high system corrosivity [30]. The lower temperature and pressure conditions required results in slower rates for hydrolysis. Furthermore, the carbonization of ethylene glycol (EG) takes place, thus affecting its purity [29,31]. Therefore, alkaline option is the most developed and desirable alternative, in which PET solid particles are hydrolyzed with an aqueous solution of NaOH or KOH (4–20 wt%) under atmospheric pressure and 80–300 ºC for several reaction hours [29]. PET reacts to produce the disodium salt (Na_2-TPA) and EG. Subsequently, pure TPA can be isolated by neutralizing the reaction mixture with a strong inorganic acid (e.g., H_2SO_4 or HCl), usually added in excess up to pH= 2–3. The yields of TPA monomer and purity of the product obtained are usually high. Several studies [10,32–37] have evidenced that some quaternary salts (QX), e.g. tetrabutyl ammonium iodide or trioctylmethylammonium bromide, which act as catalysts, can significantly accelerate the reaction rate under alkaline conditions, thereby reducing the operating temperature. Currently, no commercial-scale PET hydrolysis plant is registered. While some companies, such as Gr3n [38], Carbios [39] and Tyton Biosciences [40] are working at pilot plant scale, others have yet to disclose information on their development stage.

Among different PET products, PET bottle is one of the most recycled materials, with an average collection rate of 60% and a recycling rate of 50% in Europe, however only 31% of recycled PET from bottles is used to produce bottle pellets [1]. The rest of the recycled PET is destined to lower value products, mainly to PET trays by 31%, which are often not recycled or reused [41]. The lack of appropriate sorting and recycling technologies, as well as tray design, makes this PET waste currently difficult to recycle. Due to the variability of this type of product (color and multilayer composition) and the contamination resulting from selective or residual collection, its mechanical recycling is usually ineffective [2,42,43]. In addition, given the low intrinsic viscosity of PET trays (shorter polymer chains), mechanical recycling of PET trays into PET bottles is not viable, since the latter require a high viscosity [41]. Therefore, chemical depolymerization is being explored for PET tray valorization, since it allows to eliminate the impurities present (pigments that provide color or other types of plastics) and to produce the PET starting monomer again [22], following the principles of sustainable development in closed-loop applications [26,28,44].

Several approaches have been made to the kinetics of alkaline hydrolysis of PET using the shrinking core model. Lopez-Fonseca and coworkers [34] successfully fitted the depolymerization of PET granules to this model. Other authors have also studied the model for bottle flakes from different approaches [32,45]. However, it has not yet been tested on other types of waste.

This work aims to deepen on the valorization of monolayer PET tray waste by alkaline hydrolysis technology, under moderate operating conditions and using tributylhexadecylphosphonium bromide (TBHDPB) quaternary salt as catalyst. Particularly, the objective of this work has been focused on analyzing the effect of different operating variables (catalyst to PET ratio, PET particle size, reaction stirring rate and temperature) on PET tray waste alkaline hydrolysis, in terms of PET conversion and TPA yield. The color of the TPA obtained has also been examined owing to the interest for its industrial application. Furthermore, a kinetic model based on a shrinking core model has been proposed, which successfully fits the experimental results within a wide range of operating conditions.

2. Experimental

2.1. PET tray waste samples, chemicals and reagents

Monolayer PET tray waste come from colorless and transparent post-consumer food containers, provided by local waste management companies, after having their corresponding lids, labels and glue removed. PET samples were grounded with a knife mill (Retsch SM 300) to reduce the particle size below 2 mm. These samples were further separated based on their particle size using sieves at intervals of 9–10 mm, 1–1.4 mm and $\leq$ 0.5 mm.

Sodium hydroxide (NaOH), dimethyl sulfoxide (DMSO), tributylhexadecylphosphonium bromide (THBDPB) catalyst, potassium hydroxide (KOH) and terephthalic acid (TPA) were supplied by Sigma Aldrich (Merck).

2.2. Characterization of PET tray waste

The relative content of PET present in the samples was measured using tetrahydrofuran (THF) as solvent for 4 h at room temperature, which was able to dissolve impurities of other plastics (e.g. low density polyethylene (LDPE), polyvinyl chloride (PVC) and polystyrene (PS)) without dissolving PET. The remaining product was filtered, dried and weighed. The PVC content in PET material was quantified by heating the samples at 235 ºC for 45 min. At this temperature, PVC undergoes dehydrochlorination, releasing Cl and transforming into a polyene structure, which makes it distinguishable from other polymers due to its carbonaceous structure. Hence, PVC content was calculated based on previous calibration tests of known composition, by measuring the weight loss of the samples after Cl removal.

After cooling down, the solidified PVC adopts a carbonized black color that is easily distinguishable in order to separate it from the rest of plastic materials. PVC particles have also been identified by Fourier transform infrared spectroscopy (FTIR). PET samples' moisture and density were measured as well. The inorganic matter content was quantified by calcination of PET samples in a muffle (Nabertherm B180) at 625 ºC for 4 h, following a heating ramp of 10 ºC min^{-1}. After calcination, the remaining organic ashes were weighed and analyzed by FTIR. Both FTIR measurements were recorded using Shimadzu software in a IRAffinity equipment, MIRacle10 (diamond prism / ZnSe), in the wavenumber range of 600–4000 cm^{-1}, with a resolution of 4 cm^{-1} and with 20 scans.

Differential Scanning Calorimetry (DSC) tests were performed to measure the crystallinity of PET samples using a Mettler Toledo TGA/DSC 1 equipment, in a N_2 atmosphere with a flow of 50 mL min^{-1}. PET samples (5 mg) were heated from 20 °C to 300 °C, then cooled to 25 °C and heated again to 300 °C at a heating/cooling rate of 10 °C min^{-1}. The characteristic enthalpies and transition temperatures were calculated using the UniversalV2.6D TA Instruments software. The crystallinity of PET samples were estimated using Eq. (1) [15,46].

$$X_C = \left[\frac{(\Delta H_m - \Delta H_{cc})}{\Delta H_m^o}\right] \times 100 \quad (1)$$

where X_c is the crystallinity (%), ΔH_m (J g^{-1}) and ΔH_{cc} (J g^{-1}) are the measured melt and cold crystallization enthalpy of PET, respectively, and $\Delta H_m^o = 140.1$ J g^{-1} is the melting enthalpy of 100% crystalline PET.

2.3. Alkaline hydrolysis of PET waste

2.3.1. Reaction equipment and experimental procedure

The alkaline hydrolysis reactions of PET were carried out in a 1 L three-neck balloon-shaped reactor, equipped with a refrigeration column, a mechanical stirrer and a heating plate with a digital temperature control system, which is shown in Fig. S1 (Supporting Information). In a typical experiment, NaOH (46.6 g), water (666.6 g) and TBHDPB catalyst (3.3–13.2 g) were fed to the reactor and then heated up to the specific reaction temperature (80–100 °C). Once this reaction temperature is reached, PET flakes (66.6 g) were added to the reaction mixture.

In the reaction stage, PET reacts to produce the disodium salt (Na_2-TPA) and ethylene glycol (EG) according to Eq. (2).

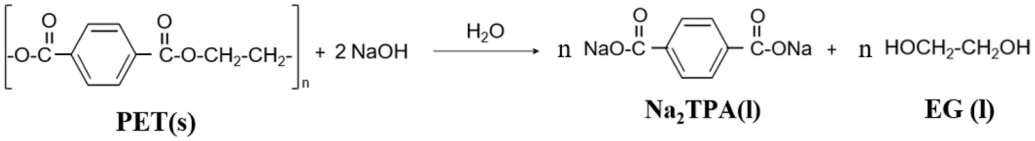

(2)

Throughout the 4 h reaction time interval, 15 mL samples were taken every 0.5, 1, 2 and 3 h, so that the yield of TPA product over reaction time could be calculated. After the reaction, the flask was removed from the heating mantle and the hot solid-liquid mixture was filtered. The samples taken during the reaction were also hot filtered and dried at 60 ºC for 24 h. The unreacted PET solid was dried at 60 °C for 48 h. Excess sulfuric acid was added into disodium terephthalate (Na_2-TPA) solution until pH= 2–3 was reached, thus provoking the precipitation of the acid monomer to solid terephthalic acid (TPA), following the reaction described in Eq. (3) [32].

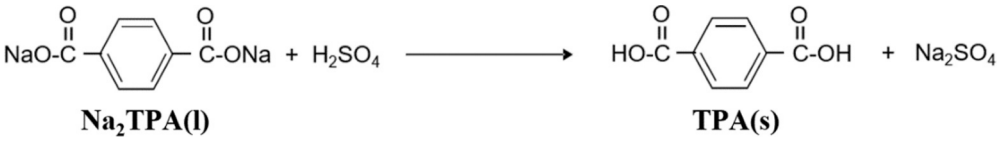

(3)

Once the precipitation was completed, the solid product was filtered in order to recover the TPA product for its analysis. The filtrate was essentially composed of ethylene glycol, the quaternary salt, salts generated during the neutralization step and water. It should be mentioned that an excess of sulfuric acid resulted in the formation of sodium sulfate salt (Na_2SO_4) [47]. Therefore, all the samples were washed with deionized water using approximately twice the neutralized volume. Recovered TPA was dried at 60 °C until no change in weight was observed. The transformation of Na_2TPA into TPA product was also checked by means of FTIR analysis.

Fig. 1 shows schematically the methodology carried out for the reaction of PET and the neutralization and purification of TPA product.

2.3.2. TPA product characterization

In order to calculate the purity of the TPA obtained, a calibration was performed using standard TPA, thus establishing the relationship between the amount of potassium hydroxide needed to neutralize known amounts of reference TPA (purity 98%). This calibration curve is shown in Fig. S2a (Supporting Information). For this purpose, 0–0.1 g of TPA were dissolved in 15 mL of dimethyl sulfoxide (DMSO), titrated with 0.1 N KOH solution to a phenolphthalein endpoint. DMSO and ionic liquids (e.g. 1-butyl-3-methylimidazolium acetate and 1-ethyl-3-methyl-iminidazolium) are an alternative to pyridine as green solvents [48,49]. The experimental purity was determined using 0.05 and 0.08 g of TPA samples and using the same amount of solvent, titrant and indicator as for reference calibration. The purity of the samples was determined using Eq. (4).

$$\text{Purity} = \frac{1}{127}\frac{\text{Volumen of solution KOH 0.1M (mL)}}{\text{Sample weight (g)}} \quad (4)$$

Due to the pigments and colorants added during PET processing, PET depolymerization can also lead to a colored TPA monomer, which polymerization will in turn produce a colored rPET [50,51]. Furthermore, the presence of color in rPET can also limit its application and viability in comparison to commercial PET [52,53]. Hence, a characterization of the color of TPA produced after PET hydrolysis was also carried out using a CM-2300d model spectrophotometer with a wavelength range between 360 nm and 740 nm. The CIE 1976 L*a*b* (CIELAB) color space was used, which defines the color of an object through three parameters: L* (100 = white; 0 = black), a* (positive = red; negative = green; 0 = gray) and b* (positive = yellow; negative = blue; 0 = gray) (Fig. S2b). The difference in color observed between the TPA produced in the depolymerization with respect to the standard TPA is determined according to the Eq. (5) [54].

$$\Delta E = \sqrt{(L^*)^2 + (a^*)^2 + (b^*)^2} \quad (5)$$

where ΔE is the color difference. A threshold value of $\Delta E \leq 15$ was set as the appropriate color value for the TPA produced with respect to the colorless synthetic TPA, used as reference material.

2.3.3. Operating conditions and reaction indices

To study the alkaline hydrolysis of PET, the tests described in Table 1 were carried out at atmospheric pressure. The kinetic results obtained have allowed studying the following effects: (i) TBHDPB catalyst to PET mass ratio (0, 0.05, 0.1 and 0.2); (ii) PET particle size (≤0.5 mm, 1–1.4 mm and 9–10 mm); (iii) stirring rate (350, 525 and 700 rpm); (iv) temperature (80, 90 and 100 °C). In addition, PET depolymerization tests were performed at 0.5, 1 and 2 h, in order to obtain additional data for the development of the kinetic model described in Section 2.4. The

Fig. 1. Depolymerization stage followed by purification steps for the alkaline hydrolysis of PET to TPA.

Table 1
Experimental conditions for alkaline hydrolysis runs at atmospheric pressure.

T (ºC)	TBHDPB:PET (wt%)	Particle size (mm)	Stirring rate (rpm)	Reaction time (h)
100	0	1–1.4	525	0.5/1/2/4
100	0.05	1–1.4	525	0.5/1/2/4
100	0.1	1–1.4	525	0.5/1/2/4
100	0.2	1–1.4	525	0.5/1/2/4
100	0.1	9–10	525	4
100	0.1	≤ 0.5	525	4
100	0.1	1–1.4	350	4
100	0.1	1–1.4	700	4
80	0.1	1–1.4	525	4
90	0.1	1–1.4	525	4
80	0	1–1.4	525	4
90	0	1–1.4	525	4

reaction tests were carried out in duplicate.

The results were evaluated in terms of PET conversion and TPA yield. PET conversion was gravimetrically determined on the basis of the weights of unreacted PET material (Fig. 1) using Eq. (6) [15].

$$PET_{conversion}(\%) = \frac{W^0_{PET} - W^t_{PET}}{W^0_{PET}} \cdot 100 \tag{6}$$

where W^0_{PET} (g) and W^t_{PET} (g) refer to initial weight of PET fed and PET weight at a specific reaction time, respectively.

By establishing TPA weight and purity for each kinetic run (Fig. 1), TPA yield can be calculated as shown in Eq. (7) [32].

$$TPA_{yield}(\%) = \frac{W^t_{TPA}/MW_{TPA}}{W^0_{PET}/MW_{PET}} \cdot Purity \cdot 100 \tag{7}$$

where W^t_{TPA} (g) and W^0_{PET} (g) refer to the weight of TPA at a specific reaction time and the initial weight of PET, respectively. MW_{TPA} and MW_{PET} are the molecular weights of TPA (166 g mol^{-1}) and PET monomer (192 g mol^{-1}), respectively.

2.4. Methodology for the kinetic model

For the development of a kinetic model of the catalytic depolymerization of PET tray waste, a shrinking core model has been proposed. The selection of this type of model is based on the following premises: (i) Heterogeneous solid-liquid nature of the reaction; (ii) No solid products are produced that could remain on the PET particle surface; and, (iii) PET polymer is a non-porous and insoluble material in the reaction mixture.

This model assumes that there is no appreciable diffusion of ion pair (reaction anion (OH^-) and cation (Q^+)) in the interior of the PET particle; and, therefore, that the reaction occurs on the external surface [34, 55]. The extent of the reaction within the core of the PET particle was assumed to be negligible. Hence, the achieved conversion can be related to the radius of the particle as shown in Eq. (8) [56].

$$N_{PET} = \rho_{PET} V_{PET} \tag{8}$$

where V_{PET} is the volume of the PET particle and ρ_{PET} is the density of the PET. For the mathematical treatment, it was assumed that PET samples consist of isotropic spherical particles of equal diameter. The particle size of PET is small enough (1.2 mm) that PET particles can be reasonably assumed to be spherical in shape. Therefore, the conversion of PET can be defined as shown in Eq. (9) [56].

$$X = \frac{N_{PET_0} - N_{PET}}{N_{PET_0}} = \frac{\rho_{PET}\left(\frac{4}{3}\pi R_0^3\right) - \rho_{PET}\left(\frac{4}{3}\pi R^3\right)}{\rho_{PET}\left(\frac{4}{3}\pi R_0^3\right)} = 1 - \left(\frac{R}{R_0}\right)^3 \tag{9}$$

where R is the radius of PET particle for a given time (t), R_0 is the initial radius of PET particle and X is PET conversion.

Furthermore, the kinetics of ion exchange and the external diffusion of the TBHDPB catalytic entity from the liquid phase to the external surface of the solid reagent are considered to be very fast, so that the depolymerization of PET under alkaline conditions is entirely controlled by the chemical reaction [34]. This assumption is based on the use of a phase catalyst (TBHDPB), which significantly favors external diffusion. Additionally, in prior studies in the literature it was observed that in the absence of catalyst, an increase in temperature gave way to a substantial increase in PET conversion [33]. Under these conditions, the disappearance rate of PET will be exclusively a function of the reaction rate. Therefore, the concentration of sodium hydroxide (C_{NaOH}) at the surface will be constant and equal to the concentration of the feed (C_{NaOH0}). For a spherical particle, the reaction rate can be written as Eq. (10).

$$-\frac{dN_{NaOH}}{dt} = \left(-r_{NaOH}\right)_{sup} * \left(4\pi R_C^2\right) \tag{10}$$

where $(-r_{NaOH})_{sup}$ is the rate of reaction per unit contact area. For a general kinetic expression, the global reaction rate will be that corresponding to the sum of the reaction in the presence of phase catalyst and when it occurs spontaneously, without the participation of the TBHDPB catalyst (Eq. (11)).

$$\left(-r_{NaOH}\right)_{sup} = k_{esp} C_{NaOH} + k_{QX} C_{QX} C_{NaOH} = C_{NaOH}\left(k_{esp} + k_{QX} C_{QX}\right) = C_{NaOH} k' \tag{11}$$

where k_{esp} is the intrinsic non-catalytic depolymerization rate constant, k_{QX} is the catalyzed depolymerization rate constant and k' is the apparent rate constant, which depends linearly on the concentration of the TBHDPB quaternary salt (C_{QX}).

Considering the stoichiometry of the reaction of 2 moles of NaOH per 1 monomer of PET, the rate of disappearance of PET can be evaluated as shown in Eq. (12).

$$-\frac{dN_{PET}}{dt}=\frac{1}{2}\left(4\pi R^2\right)C_{NaOH}k' \tag{12}$$

where N_{PET} is the number of repeating unit moles of PET and R is the average radius of the unreacted PET particles. The reversible decomposition reaction of PET is neglected since, as the reaction proceeds, the produced TPA dissolves in solution as Na_2-TPA. Hence, TPA will be inactive in an eventual nucleophilic substitution for the esterification (the reverse reaction for alkaline hydrolysis) [34,57]. The reaction rate is proportional to the surface area of the particle, the OH^- concentration, and the QX concentration.

By differentiating, rearranging and substituting Eq. (9) in Eq. (12), Eq. (13) and Eq. (14) are obtained. More details on the mathematical procedure are shown in the Supporting Information.

$$\frac{dX}{dt}=k''(M-2X)(1-X)^{\frac{2}{3}} \tag{13}$$

$$k''=\frac{3C_{PET_0}}{2\rho_{PET}R_0}(k_{esp}+k_{QX}C_{QX}) \tag{14}$$

By integrating Eq. (13) for the initial conditions of ($t=0$ when $X=0$), for $M>2$, and further rearranging, Eq. (15) is obtained [55]:

$$\begin{aligned} f(x)&=\frac{1}{4c^2}\ln\left[\frac{(c+z)^3}{c^3+z^3}\right]+\frac{\sqrt{3}}{2c^2}\arctan\left(\frac{2z-c}{c\sqrt{3}}\right)\\ &=-kt+\frac{1}{4c^2}\ln\left[\frac{(c+1)^3}{c^3+1}\right]+\frac{\sqrt{3}}{2c^2}\arctan\left(\frac{2-c}{c\sqrt{3}}\right)\end{aligned} \tag{15}$$

where

$$c^3=\left[\frac{M-2}{2}\right] \tag{16}$$

$$z=(1-x)^{\frac{1}{3}} \tag{17}$$

Eq. (15) predicts the evolution of PET conversion with reaction time for different TBHDPB:PET feed ratios. The slope of this linear equation corresponds to the apparent kinetic constant k''.

3. Results

3.1. Characterization of PET tray waste

Table S1 (Supporting Information) summarizes the main properties of as-received PET tray waste prior to reaction. PET tray waste shows a 98.94 wt% of PET content with small amounts of moisture (0.83 wt%), inorganic compounds (0.2 wt%) and PVC (8.22 ppm), which is significantly lower than the maximum PVC content (200 ppm) allowed for PET production [58].

Fig. S3 (Supporting Information) shows the FTIR spectrum of the virgin tray material. This displayed the typical bands of PET [59], namely 1712 cm^{-1} (C═O stretching of the carboxylic acid group), 1410–1338 cm^{-1} (stretching of the C-O group, deformation of the O-H group and bending vibrational modes and oscillation of the ethylene glycol segment), 1240 cm^{-1} (terephthalate group, $OOCC_6H_4$- COO), 1090–1030 cm^{-1} (methylene group and vibrations of the C-O ester bond) and 720 cm^{-1} (interaction of polar ester groups and benzene rings).

As previously mentioned, the chemical nature of the inorganic compounds present after the calcination of PET samples was also characterized by FTIR. The following characteristic bands were identified (Fig. S4, Supporting Information): silica compounds, in the 1000–1100 cm^{-1} range, which was accompanied by the band at 670 cm^{-1}, showing the existence of silicon oxide compounds or silicates. In addition, the band at 800–700 cm^{-1} attributable to antimony and tin oxide compounds was also detected. Antimony oxides are normally used in plastic compounds as flame retardants [60]. Moreover, the bands of calcium carbonate were observed (1400 and 870 cm^{-1}). These bands represent the union of CO_3^{2-} associated with calcite [59]. The addition of calcium carbonate in PET plastics improves the thermal stability of the matrix [61].

The crystallinity values obtained from the DSC profile depicted in Fig. S5 (Supporting Information) are also listed in Table S1. The extrinsic crystallinity corresponds to scan 3, once the thermal history from the shaping of the material has been eliminated. The intrinsic crystallinity corresponds to scan 1, where the shaping of the material modifies its base crystallinity [62]. For both tests, the crystallinities are calculated with Eq. (1) from the melt and cold crystallization enthalpies obtained from the area of the exothermic and endothermic bands of the DSC profiles, respectively. In scan 1, the following bands are visible in increasing order of temperature: an exothermic band corresponding to the transition temperature, a crystallization endothermic band and an exothermic band related to the melting of the material. Scan 3 only exhibits the exothermic melting band since the amorphous regions present by the shaping that produce the crystallization and transition bands are eliminated by scan 1.

PET tray waste samples undergo a change in heat flux in the glass transition region (75.5 ºC), which is characteristic of plastic solids with amorphous regions [63]. In addition, it exhibits an endothermic band at 129.6 ºC, assignable to the crystallization of the induced amorphous regions present in the materials [64]. The samples show a low crystallinity as a result of induced crystallization by thermal crystallization in which the polymer, after polymerization, was heated above the glass transition temperature and subsequently cooled quickly enough so that the amorphous regions did not crystallize. Therefore, the crystallinity is reduced from intrinsic to extrinsic crystallinity by 13.9%. This technique is performed to generate amorphous regions that provide some elasticity and impact resistance [63]. PET tray waste samples present a lower crystallinity than other materials such as PET fibers, which show a high crystallinity due to the stretching of the heated polymer for its shaping; or, PET bottles, which require higher crystallinities to reduce their permeability [63,64]. On the other hand, it must be stated that the melting temperature of the PET samples was 248.3 °C.

3.2. Effect of the operating variables on the hydrolysis of monolayer PET tray waste

3.2.1. Effect of catalyst:PET ratio

Fig. 2 shows the effect of the TBHDPB catalyst to PET feed (TBHDPB:PET) mass ratio on PET conversion (Fig. 2a) and TPA yield (Fig. 2b) over reaction time at 100 ºC.

In the absence of catalyst (TBHDPB:PET= 0), the evolution of PET conversion over time (Fig. 2a) is notably lower than that found when various catalyst-PET ratios are used. Furthermore, with no catalyst the conversion increases almost linearly from a value of 7% for t = 0.5 h to a value of 34% for t = 4 h, while the addition of the catalyst leads to an exponential increase in conversion with time. This is justified because without the presence of a phase catalyst, the hydrophobic nature of PET material limits the attack by the hydroxide ions dissolved in the aqueous phase. The catalyst reduces external diffusion limitations by increasing the contact between PET and hydroxide ion, thereby increasing PET conversion [32]. Lopez-Fonseca and co-workers [34] observed that the complete PET conversion for alkaline hydrolysis in the absence of catalyst at 80 ºC required a reaction time interval of approximately 10 h, while with a catalyst ratio of TBHDPB:PET= 0.55, led to a conversion of 95% for t = 1.5 h. In the absence of catalyst but at higher operating temperatures (180 °C), Sun and co-workers [65] also reported a PET conversion greater than 95% for t = 0.5 h.

Likewise, an increase in the TBHDPB:PET ratio promoted PET depolymerization. After 4 h, significant improvements in conversion

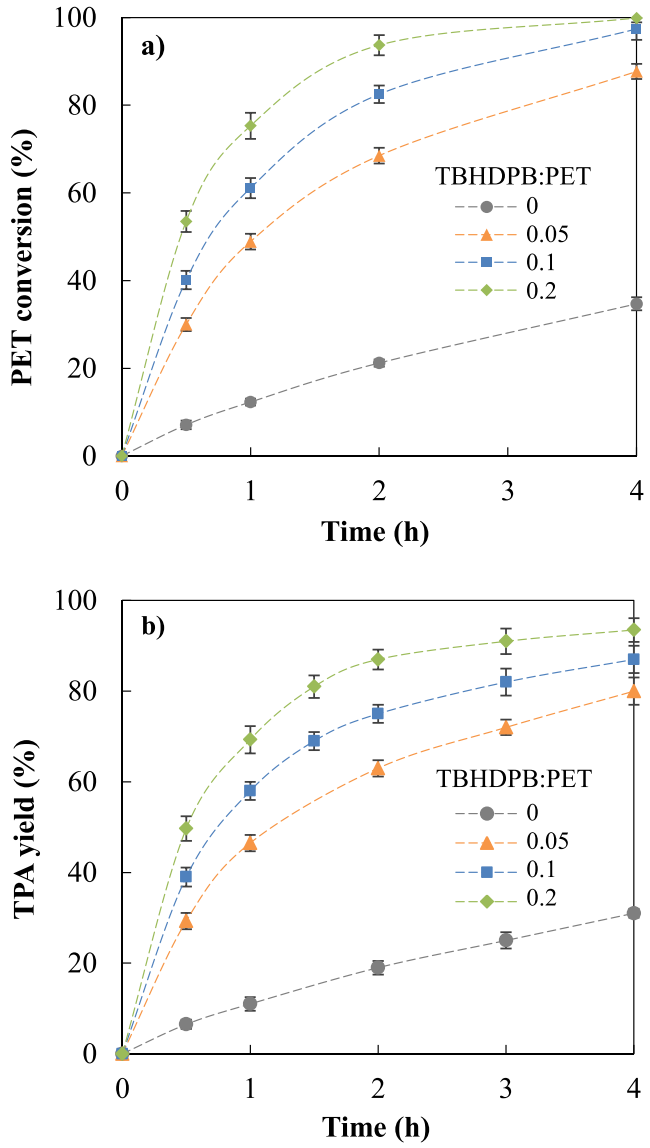

Fig. 2. Effect of the TBHDPB catalyst:PET feed ratio on the evolution with the reaction time of: a) PET conversion; and, b) TPA yield. Operating conditions: 100 ºC, particle size= 1–1.4 mm, stirring rate= 525 rpm.

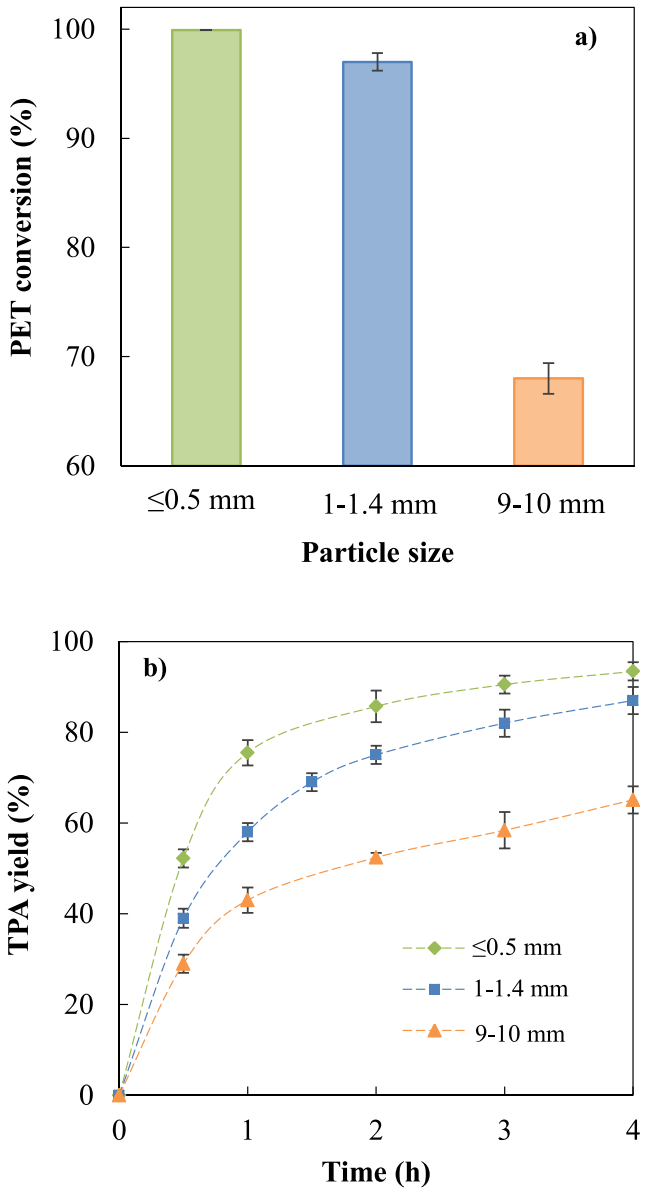

Fig. 3. Effect of PET particle size on: a) PET conversion at t = 4 h; and, b) the evolution of TPA yield with reaction time. Operating conditions: 100 ºC, TBHDPB:PET ratio= 0.1, stirring rate= 525 rpm.

were noticed, with respect to the non-catalyzed reaction, of 53%, 63.4% and 65.9% for TBHDPB:PET ratios of 0.05, 0.1 and 0.2, respectively. Almost full conversion (>98%) was obtained for TBHDPB:PET ratio of 0.1 and 0.2. Similarly, an increase in TBHDPB:PET ratio also enhanced the TPA yield (Fig. 2b), with increased values of 49.1%, 56% and 62.5% for the ratios of 0.05, 0.1 and 0.2, respectively.

3.2.2. *Effect of PET particle size*

Fig. 3 shows the effect of particle size on PET conversion after 4 h of reaction (Fig. 3a) and the evolution of TPA yield with reaction time (Fig. 3b) at 100 ºC. Both PET conversion and TPA yield increase significantly as particle size is decreased. Thus, after 4 h of reaction time, an almost complete conversion (> 97%) and a TPA yield of 93.4% are achieved for a particle size of ≤ 0.5 mm, while for an average size of 9–10 mm a conversion of 68% and a TPA yield of 65.1% are obtained. These results were expected since PET feeds with a reduced particle size show a larger available surface area; consequently, the reaction rate increased and higher PET conversions were obtained. Ügdüler and co-workers [15] obtained a similar improvement in the conversion of PET by decreasing particle size. Thus, for a size of ≤ 0.5 mm, a conversion of ~ 75% was obtained, while for a size of 9–10 mm, a conversion as low as 45% was noticed. Similarly, Mishra and co-workers [66] found that the variation in particle size between 0.3 mm and 0.6 mm had a great effect on conversion. However, Kosmidis and co-workers [32] concluded that the effect of particle size on PET conversion for the studied range between ≤ 0.71 mm and 2 mm, was not remarkable. Our kinetic results evidenced that decreasing the particle size of PET grains below 1 mm did not lead to a significant improvement in PET conversion. This finding was highly relevant for the industrial implementation of PET alkaline hydrolysis since cost associated with energy-intensive grinding to lower sizes could be partially avoided [15, 67,68].

3.2.3. *Effect of stirring rate*

Fig. 4 shows the effect of stirring rate on PET conversion after 4 h of reaction time (Fig. 4a) and the evolution over time of TPA yield (Fig. 4b) at 100 ºC. PET conversion increases progressively with stirring rate from

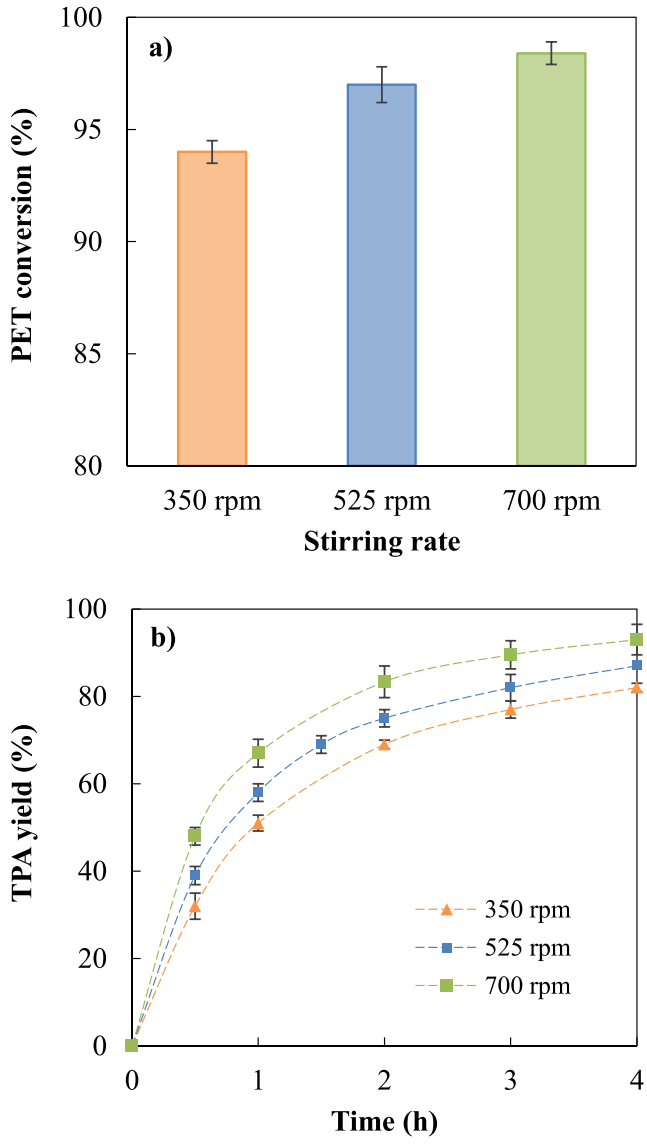

Fig. 4. Effect of stirring rate on: a) PET conversion at reaction time= 4 h; and, b) the evolution with time of TPA yield. Operating conditions: 100 ºC, particle size= 1–1.4 mm, TBHDPB:PET ratio= 0.1.

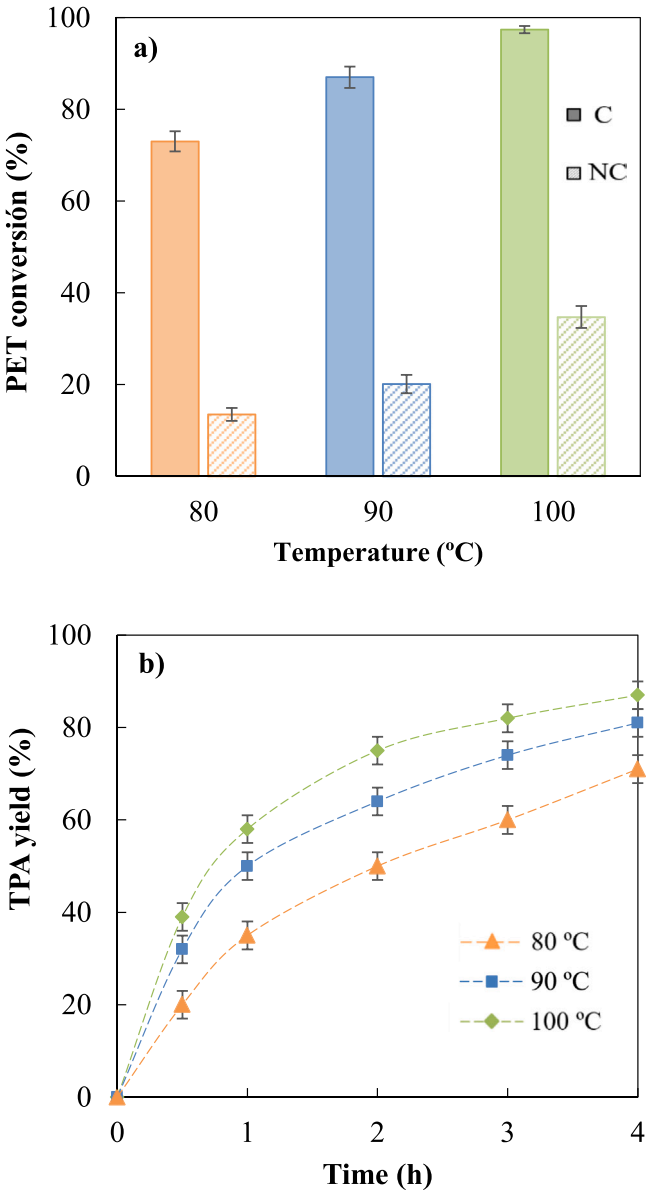

Fig. 5. Effect of reaction temperature on: a) PET conversion at reaction time= 4 h (C= Catalyzed and NC= Non-catalyzed); and, b) the evolution with reaction time of TPA yield. Operating conditions: particle size= 1–1.4 mm, TBHDPB:PET ratio= 0.1, stirring rate= 525 rpm.

94% for 350 rpm to 98.4% for 700 rpm. These results followed a similar trend to those obtained by Ügdüler and co-workers [15], who observed a notable increase in PET conversion, from 33.7% for 250 rpm to 70.5% for 500 rpm during alkaline hydrolysis at 80 ºC. The stirring rate mainly affects external diffusion (mass transfer between solid and liquid phase), which is the controlling step for alkaline hydrolysis in the absence of catalyst, thus decreasing reaction time. Sun and co-workers [65] found out that for high temperatures (180 ºC) and for a reaction time where full PET conversion was achieved, stirring rate had no significant effect on TPA yield or purity, which evidenced that stirring only had a positive effect on limiting mass and temperature diffusional controls, thus increasing reaction kinetics.

3.2.4. *Effect of reaction temperature*

Fig. 5 compares the effect of temperature on PET conversion (Fig. 5a) for t = 4 h in the presence and absence of catalyst and on TPA yield over reaction time (Fig. 5b). A direct and proportional increase in PET conversion was observed while increasing temperature, for both non-catalyzed and catalyzed reactions. As previously discussed in Section 3.2.1, in the absence of catalyst PET conversions were notably lower than those obtained using TBHDPB catalyst for the studied temperature range. A less marked effect of temperature on PET conversion for the non-catalyzed reaction was expected, as the reaction was controlled by external diffusion [29]. However, a raise in temperature provoked an exponential increase in PET conversion, from 13.5% at 80 ºC to 25% at 100 ºC. When TBHDPB is used as catalyst, the conversion increases from 85.8% at 80 ºC up to 97% at 100 ºC. TPA yield (Fig. 5b) also increased significantly with temperature, reaching a maximum TPA yield after 4 h of reaction time of 87% at 100 ºC.

These results highlighted the significant role played by temperature, where an increase in temperature results in higher depolymerization kinetic constants (k'). Furthermore, the depolymerization reaction of PET is an endothermic process and, thus, an increase in temperature promotes its decomposition. Ügdüler and co-workers [15], observed that at low reaction temperatures (50 ºC), the thermal energy was insufficient to activate the hydrolysis of PET. On the other hand, at high temperatures (>180 ºC), secondary reactions such as thermal oxidative

degradation of PET and intermolecular dehydration of ethylene glycol can be favored, thereby making subsequent purification operations more difficult [65].

3.3. TPA product characterization

Fig. S6 (Supporting Information) illustrates the unreacted PET tray cake, the separated unreacted filtrate, and the neutralized solid TPA product after filtration. Despite the intense color of the filtered product, after neutralization with sulfuric acid and filtering, the final product loses much of its color.

The transformation of Na_2TPA into TPA after acidification was confirmed by FTIR analysis (Fig. S7, Supporting Information). Characteristic absorption peaks were observed at 3018 cm^{-1}, 2804 cm^{-1} and 2549 cm^{-1} corresponding to carboxylic groups. The signals at 1693 cm^{-1}, 1300 cm^{-1} and 1420 cm^{-1} are related to the carbonyl group. The characteristic peaks corresponding to the aromatic rings were noted in the region of 700–800 cm^{-1} [37,67]. Furthermore, the difference in color between the TPA produced from the depolymerization of the PET tray and the reference TPA turned out to be adequate with ΔE values below 3.6 under the investigated reaction conditions, which is indeed a clear advantage for the subsequent polymerization of TPA to colorless plastics, especially demanded in the food sector. The CIELAB parameters are shown in Table S1 (Supporting Information).

3.4. Kinetic parameters and model validation

Fig. 6a shows the evolution over reaction time of the *f(x)* function, described in Eq. (15), fordifferent TBHDPB:PET ratios at 100 °C. The usefulness of the proposed shrinking core model is validated by evaluating the left hand side of Eq. (15), which is a function of PET conversion *f(x)*, and subsequent plotting against the reaction time by varying concentration of the quaternary phosphonium salt. The slope of the corresponding linear plot corresponds to the apparent kinetic constant *k''*.

A fit of the model to the experimental data with correlation factors (r^2) greater than 0.99 were obtained for all the kinetic runs. Therefore, the proposed kinetic model adequately represents the alkaline hydrolysis of PET tray waste in the presence of the TBHDPB catalyst. In addition, Fig. 7 shows the relationship of the apparent rate constant (k') with varying TBHDPB:PET ratios, thus concluding that alkaline hydrolysis fits to a first order reaction with respect to concentration of

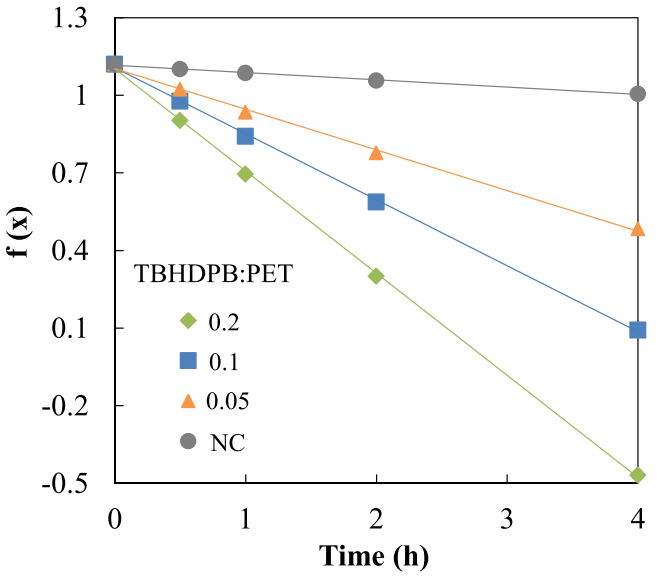

Fig. 6. Fitting of kinetic data according to Eq. (15) at 100 °C and different TBHDPB:PET ratios.

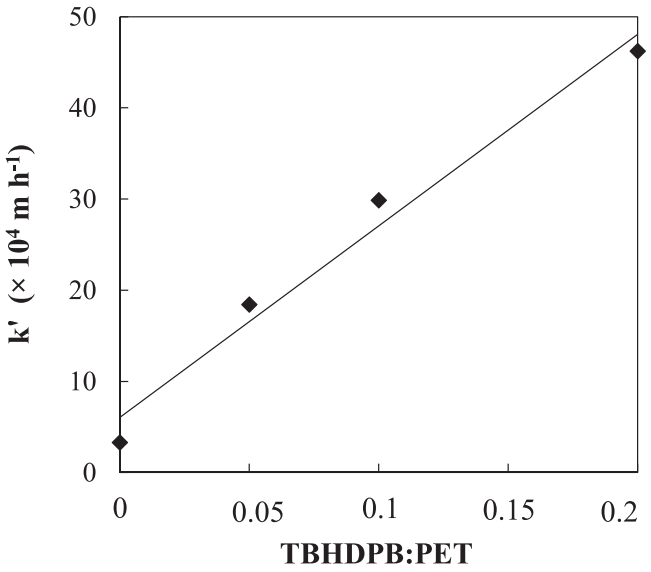

Fig. 7. Linearization of apparent rate constants (k') with catalyst concentration.

Table 2
Kinetic parameters for alkaline hydrolysis of PET for different TBHDPB:PET ratios and different temperatures.

TBHDPB:PET		T = 100 °C	T = 90 °C	T = 80 °C
0	k'' (×10² h^{-1})	2.82	1.35	0.95
	k_{esp} (×10⁴ m h^{-1})	3.29	1.79	1.10
0.05	k'' (×10² h^{-1})	15.73	-	-
	k' (×10⁴ m h^{-1})	18.40	-	-
0.1	k'' (×10² h^{-1})	25.53	18.38	15.24
	k' (×10⁴ m h^{-1})	29.87	21.50	17.83
0.2	k'' (×10² h^{-1})	39.49	-	-
	k' (×10⁴ m h^{-1})	46.21	-	-
	k_{QX} (×10⁴ m^4 mol^{-1} h^{-1})	1.40	0.89	0.49

TBHDPB catalyst (C_{QX}) and with respect to the concentration of sodium hydroxide (C_{NaOH}).

Likewise, it was assumed that the good fitting of the proposed model at 100 °C is presumably valid at 80 °C and 90 °C. Therefore, using the conversion values at reaction time= 4 h with and without catalyst, the linear fitting to Eq. (14) at 80 °C and 90 °C is obtained, with its corresponding k'' for a TBHDPB:PET ratio of 0.1.

Table 2 includes the kinetic constants obtained from the linear regression of the values in Fig. 6 (k''), the apparent rate constants (k'), the intrinsic non-catalytic depolymerization rate constants (k_{esp}) and catalyzed depolymerization rate constants (k_{QX}). In the absence of a catalyst *k'* is equal to k_{esp}. It was found that the catalytic term of the kinetic equation (Eq. (11)) (k_{QX} C_{QX}) for the catalyst concentration range studied is between 4 and 17 times greater than the intrinsic kinetic term, so that the reaction in the absence of catalyst is kinetically relevant. This is coherent with the kinetic results obtained in the absence of catalyst (Fig. 2). López-Fonseca and co-workers [34] corroborated this same finding. Kosmidis and co-workers [32], on the other hand, observed TPA yields lower than 5% for t = 4 h, so the alkaline hydrolysis of PET in the absence of a catalyst could not be kinetically significant.

Based on the relationship of the kinetic constants (k_{esp} and k_{QX}) with temperature (Fig. 8), the activation energy was estimated from the linearized Arrhenius equation.

An apparent activation energy value of 60 and 57.4 kJ mol^{-1} was obtained for the non-catalyzed and catalyzed reactions, respectively. In view of these results, it can be concluded that TBHDPB catalyst only played an significant role in the reaction scheme by activating the

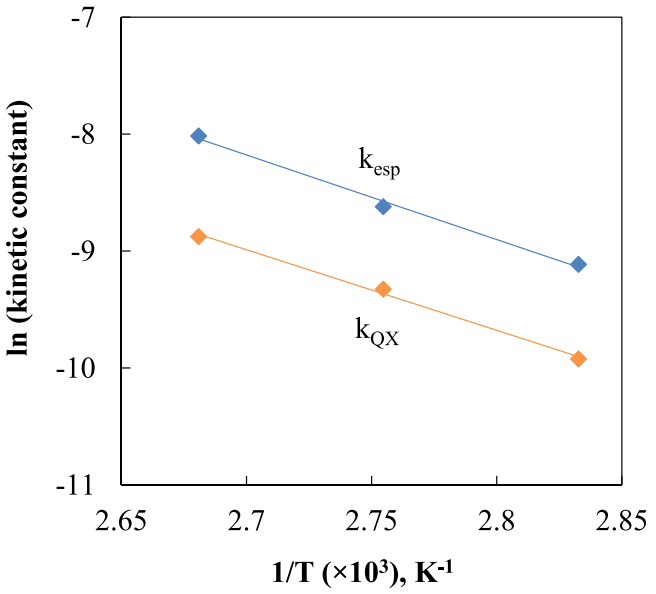

Fig. 8. Fitting to the Arrhenius equation of the kinetic constants in the absence (k_{esp}) and presence of the TBHDPB catalyst (k_{QX}) with temperature.

diffusion of hydroxide ions, apparently without modifying the reaction mechanism. This statement is supported on the basis that the activation energies in the presence and absence of catalyst are similar (Table 2), but not the TPA yields and PET conversions observed in the parametric study. Therefore, alkaline hydrolysis is controlled by external diffusion, since PET is a hydrophobic solid material, which limits the contact of hydrophilic hydroxide ions with its surface, while the TBHDPB catalyst increases the concentration of the OH^- reactant at the solid-liquid interface.

Similar results were achieved with the same catalyst in the study carried out by López-Fonseca and co-workers [34]. They obtained activation energy values of 60.6 kJ mol^{-1} and 62.6 kJ mol^{-1}, for the non-catalyzed and catalyzed reactions, respectively. Likewise, similar values were obtained in the absence of catalyst for López-Fonseca and co-workers [33] and for Mishra nad co-workers [66], reporting activation energy values of 68 kJ mol^{-1} and 59.71 kJ mol^{-1}, respectively. However, Kosmidis and co-workers [32] obtained an activation energy of 83 kJ mol^{-1} with the trioctylmethylammonium bromide (TOMAB) catalyst, concluding that the phase transfer catalyst does reduce the activation energy in reference to that obtained in the absence of catalyst by Karayannidis and co-workers [45] with a value of 99 kJ mol^{-1}. The achieved activation energy values were also lower than those attained by Siddiqui and co-workers [10] (79.2 kJ mol^{-1}) using microwave-assisted alkaline hydrolysis. It is worth pointing out that the activation energies for alkaline hydrolysis are lower than those required for acid hydrolysis: autocatalytic, 225 kJ mol^{-1} [16]; sulfuric acid, 89 kJ mol^{-1} [68]; and, nitric acid, 101 kJ mol^{-1} [69]. Activation energy values are also lower than those for neutral hydrolysis in the absence of catalyst: 123 kJ mol^{-1} [70] and 90 kJ mol^{-1} [71]. Therefore, the alkaline route is one of the most kinetically favorable processes for PET hydrolysis at present. Furthermore, alkaline hydrolysis also requires a lower activation energy than glycolysis (activation energy values greater than 85 kJ mol^{-1}) [72].

4. Conclusions

The chemical recycling of less studied PET wastes, such as PET tray wastes, by means of alkaline hydrolysis assisted by tributylhexadecylphosphonium bromide has been examined. The effect of a wide number of operating variables (temperature, concentracion of the quaternary salt, particle size and sitirring rate) has been studied. Further, kinetic data were analysed on the basis of an unreacted shriking core model. A good compromise between PET conversion (99.9%) and TPA yield (93.5%) has been established after 4 h of reaction, under the following operating conditions: catalyst ratio TBHDPB:PET= 0.2:1; T = 100 ºC; particle size= 1–1.4 mm and stirring rate= 525 rpm.

In the absence of a phase transfer catalyst and for moderate temperatures (80–100 °C), the depolymerization of PET by alkaline hydrolysis is a slow process which is limited by mass transfer between the aqueous phase and PET. Particularly, under the conditions studied, the catalytic term (k_{QX} C_{QX}) is between 4 and 17 times higher than the intrinsic kinetic term (k_{esp}). Therefore, an increase in catalyst to PET ratio leads to an increase in PET conversion and TPA yield. Likewise, an increase in the stirring rate and a decrease in the particle size result in higher PET depolymerization rate since external diffusion limitations are reduced to some extent. Likewise, an increase in temperature also favors the chemical reaction rate.

The experimental kinetic data fits suitably to the proposed shrinking core model. It has been proved that the alkaline hydrolysis of PET is a first order reaction with respect to sodium hydroxide concentration (C_{NaOH}) and catalyst concentration (C_{QX}). Furthermore, similar activation energies have been obtained for the catalyzed (57.4 kJ mol^{-1}) and non-catalyzed (60 kJ mol^{-1}) reactions. Consequently, the catalyst only favors external diffusion of the hydroxide ion, without modifying the reaction mechanism.

CRediT authorship contribution statement

Asier Barredo: Investigation, Writing – original draft, Conceptualization, Methodology, Visualization, **Asier Asueta:** Conceptualization, Validation, Investigation, Supervision, **Izotz Amundarain:** Investigation, Data Curation, Methodology, **Jon Leivar:** Investigation, Data Curation, Methodology, **Rafael Miguel-Fernández:** Project administration, Supervision, Funding acquisition, **Sixto Arnaiz:** Project administration, Supervision, Funding acquisition, **Eva Epelde:** Writing – original draft, Visualization, Conceptualization, Supervision, **Rubén López-Fonseca:** Writing – review & editing, Methodology, Formal analysis **Jose Ignacio Gutiérrez-Ortiz:** Writing – review & editing, Methodology, Formal analysis.

Declaration of Competing Interest

The authors declare that they have no known competing financial interests or personal relationships that could have appeared to influence the work reported in this paper.

Data Availability

The authors are unable or have chosen not to specify which data has been used.

Acknowledgments

This work has been developed at GAIKER Technology Centre and funded by the Department of Economic Development, Sustainability and Environment of the Basque Government by its ELKARTEK 2020 Program (NEOPLAST Project, Reference KK-2020/00107) and also by CDTI (Centro para el Desarrollo Tecnológico Industrial), within the framework of grants for Technological Centers of Excellence “Cervera” (OSIRIS Project, CER-20211009).

Appendix A. Supporting information

Supplementary data associated with this article can be found in the online version at doi:10.1016/j.jece.2023.109823.

References

[1] A. Bolanle, Z. Zainon, A. Hassan, M. Kamaruddin, A. Hamid, S. Amril, A. Hussein, Current developments in chemical recycling of post-consumer polyethylene terephthalate wastes for new materials production: A review, J. Clean. Prod. 225 (2019) 1052–1064, https://doi.org/10.1016/j.jclepro.2019.04.019.

[2] C.T. de, M. Soares, M. Ek, E. Östmark, M. Gällstedt, S. Karlsson, Recycling of multi-material multilayer plastic packaging: Current trends and future scenarios, Resour. Conserv. Recycl. 176 (2022), 105905, https://doi.org/10.1016/j.resconrec.2021.105905.

[3] J. Huang, A. Veksha, W.P. Chan, A. Giannis, G. Lisak, Chemical recycling of plastic waste for sustainable material management: A prospective review on catalysts and processes, Renew. Sustain. Energy Rev. 154 (2022), 111866, https://doi.org/10.1016/j.rser.2021.111866.

[4] European Parliament, Directive (Eu) 2019/904 of the European Parliament and of the Council of 5 June 2019 on the reduction of the impact of certain plastic products on the environment. (2019). ⟨https://eur-lex.europa.eu/eli/dir/2019/904/oj⟩, (accessed 15 April 2022).

[5] CIDEC, RPET. (2020). ⟨http://somoscidec.com/la-letra-que-lo-cambia-todo/wp-content/uploads/2021/01/Informe.pdf⟩, (accessed 12 March 2022).

[6] UNEP, Single-use plastic bottles and their alternatives. (2020). ⟨https://www.lifecycleinitiative.org/wp-content/uploads/2020/07/UNEP_PLASTIC-BOTTLES-REPORT_29-JUNE-2020_final-low-res.pdf⟩, (accessed 15 February 2022).

[7] F. Times, Recycled plastic prices double as drinks makers battle for supplies. ⟨https://www.ft.com/content/122e7584-c837–44bc-9965–9fd37d7c03ca⟩, (accessed 15 June 2022).

[8] F. Report, T. European, C. Agency, Chemical Recycling of Polymeric Materials from Waste in the Circular Economy. (2021). ⟨https://echa.europa.eu/documents/10162/1459379/chem_recycling_final_report_en.pdf/887c4182–8327-e197–0bc4–17a5d608de6e⟩, (accessed 22 February 2022).

[9] V. Sinha, M.R. Patel, J.V. Patel, Pet waste management by chemical recycling: A review, J. Polym. Environ. 18 (2010) 8–25, https://doi.org/10.1007/s10924-008-0106-7.

[10] M.N. Siddiqui, D.S. Achilias, H.H. Redhwi, D.N. Bikiaris, K.A.G. Katsogiannis, G. P. Karayannidis, Hydrolytic depolymerization of PET in a microwave reactor, Macromol. Mater. Eng. 295 (2010) 575–584, https://doi.org/10.1002/mame.201000050.

[11] N.A.S. Suhaimi, F. Muhamad, N.A. Abd Razak, E. Zeimaran, Recycling of polyethylene terephthalate wastes: A review of technologies, routes, and applications, Polym. Eng. Sci. 62 (2022) 2355–2375, https://doi.org/10.1002/pen.26017.

[12] F. Zhang, F. Wang, X. Wei, Y. Yang, S. Xu, D. Deng, Y.-Z. Wang, From trash to treasure: Chemical recycling and upcycling of commodity plastic waste to fuels, high-valued chemicals and advanced materials, J. Energy Chem. 69 (2022) 369–388, https://doi.org/10.1016/j.jechem.2021.12.052.

[13] J. Xin, Q. Zhang, J. Huang, R. Huang, Q.Z. Jaffery, D. Yan, Q. Zhou, J. Xu, X. Lu, Progress in the catalytic glycolysis of polyethylene terephthalate, J. Environ. Manag. 296 (2021), 113267, https://doi.org/10.1016/j.jenvman.2021.113267.

[14] A. Aguado, L. Martínez, L. Becerra, M. Arieta-araunabeña, S. Arnaiz, A. Asueta, I. Robertson, Chemical depolymerisation of PET complex waste: hydrolysis vs. glycolysis, J. Mater. Cycles Waste Manag 16 (2014) 201–210, https://doi.org/10.1007/s10163-013-0177-y.

[15] S. Ügdüler, K.M. Van Geem, R. Denolf, M. Roosen, N. Mys, K. Ragaert, S. De Meester, Towards closed-loop recycling of multilayer and coloured PET plastic waste by alkaline hydrolysis, Green Chem. 22 (2020) 5376–5394, https://doi.org/10.1039/d0gc00894j.

[16] W. Yang, R. Liu, C. Li, Y. Song, C. Hu, Hydrolysis of waste polyethylene terephthalate catalyzed by easily recyclable terephthalic acid, Waste Manag 135 (2021) 267–274, https://doi.org/10.1016/j.wasman.2021.09.009.

[17] K. Chan, A. Zinchenko, Conversion of waste bottles' PET to a hydrogel adsorbent via PET aminolysis, J. Environ. Chem. Eng. 9 (2021), 106129, https://doi.org/10.1016/j.jece.2021.106129.

[18] K. Chan, A. Zinchenko, Conversion of waste bottle PET to magnetic microparticles adsorbent for dye-simulated wastewater treatment, J. Environ. Chem. Eng. 10 (2022), 108055, https://doi.org/10.1016/j.jece.2022.108055.

[19] S. Tang, F. Li, J. Liu, B. Guo, Z. Tian, J. Lv, MgO/NaY as modified mesoporous catalyst for methanolysis of polyethylene terephthalate wastes, J. Environ. Chem. Eng. 10 (2022), 107927, https://doi.org/10.1016/j.jece.2022.107927.

[20] J. Payne, M.D. Jones, The chemical recycling of polyesters for a circular plastics economy: challenges and emerging opportunities, ChemSusChem 14 (2021) 4041–4070, https://doi.org/10.1002/cssc.202100400.

[21] S. Hann, T. Connock, Chemical Recycling: State of Play Report for CHEM Trust, (2020). ⟨https://www.eunomia.co.uk/reports-tools/final-report-chemical-recycling-state-of-play/⟩, (accessed 26 February 2022).

[22] M. Han, Depolymerization of PET Bottle via Methanolysis and Hydrolysis, Plast. Des. Lib. (2019) 85–108, https://doi.org/10.1016/b978-0-12-811361-5.00005-5.

[23] Infinite Loop. ⟨https://www.loopindustries.com/cms/wp-content/uploads/2021/08/Loop-Industries-Investor-Presentation_Final.pdf⟩, (accessed 21 March 2022).

[24] B. Geyer, G. Lorenz, A. Kandelbauer, Recycling of poly(ethylene terephthalate) – A review focusing on chemical methods, Express Polym. Lett. 10 (2016) 559–586, https://doi.org/10.3144/expresspolymlett.2016.53.

[25] F. Kawai, The current state of research on PET hydrolyzing enzymes available for biorecycling, Catalysts 11 (2021) 206, https://doi.org/10.3390/catal11020206.

[26] M. Dębowski, A. Iuliano, A. Plichta, S. Kowalczyk, Z. Florjańczyk, Chemical recycling of polyesters, Polim. /Polym. 64 (2019) 764–776, https://doi.org/10.14314/POLIMERY.2019.11.5.

[27] M.J. Kang, H.J. Yu, J. Jegal, H.S. Kim, H.G. Cha, Depolymerization of PET into terephthalic acid in neutral media catalyzed by the ZSM-5 acidic catalyst, Chem. Eng. J. 398 (2020), 125655, https://doi.org/10.1016/j.cej.2020.125655.

[28] J. Jiang, K. Shi, X. Zhang, K. Yu, H. Zhang, J. He, Y. Ju, J. Liu, From plastic waste to wealth using chemical recycling: A review, J. Environ. Chem. Eng. 10 (2022), 106867, https://doi.org/10.1016/j.jece.2021.106867.

[29] E. Barnard, J.J. Rubio Arias, W. Thielemans, Chemolytic depolymerisation of PET: A review, Green. Chem. 23 (2021) 3765–3789, https://doi.org/10.1039/d1gc00887k.

[30] A.B. Raheem, Z.Z. Noor, A. Hassan, M.K. Abd Hamid, S.A. Samsudin, A.H. Sabeen, Current developments in chemical recycling of post-consumer polyethylene terephthalate wastes for new materials production: A review, J. Clean. Prod. 225 (2019) 1052–1064, https://doi.org/10.1016/j.jclepro.2019.04.019.

[31] A.M. Al-Sabagh, F.Z. Yehia, G. Eshaq, A.M. Rabie, A.E. ElMetwally, Greener routes for recycling of polyethylene terephthalate, Egypt. J. Pet. 25 (2016) 53–64, https://doi.org/10.1016/j.ejpe.2015.03.001.

[32] V.A. Kosmidis, D.S. Achilias, G.P. Karayannidis, Poly(ethylene terephthalate) recycling and recovery of pure terephthalic acid. Kinetics of a phase transfer catalyzed alkaline hydrolysis, Macromol. Mater. Eng. 286 (2001) 640–647, https://doi.org/10.1002/1439-2054(20011001)286:10<640::AID-MAME640>3.0.CO;2-1.

[33] R. López-Fonseca, M.P. González-Marcos, J.R. González-Velasco, J.I. Gutiérrez-Ortiz, Chemical recycling of PET by alkaline hydrolysis in the presence of quaternary phosphonium and ammonium salts as phase transfer catalysts, WIT Trans. Ecol. Environ. 109 (2008) 511–520, https://doi.org/10.2495/WM080521.

[34] R. López-Fonseca, J.R. González-Velasco, J.I. Gutiérrez-Ortiz, A shrinking core model for the alkaline hydrolysis of PET assisted by tributylhexadecylphosphonium bromide, Chem. Eng. J. 146 (2009) 287–294, https://doi.org/10.1016/j.cej.2008.09.039.

[35] M.C.D. Spaseska, Nalkaline hydrolysis of poly(ethylene terephthalate) recycled from the postconsumer soft-drink bottles, D. Spaseska, M. Civkaroska 379 J, Univ. Chem. Technol. Metall. 45 (2010) 379–384.

[36] A. Palme, A. Peterson, H. de la Motte, H. Theliander, H. Brelid, Development of an efficient route for combined recycling of PET and cotton from mixed fabrics, Text. Cloth. Sustain. 3 (2017) 2197–9936, https://doi.org/10.1186/s40689-017-0026-9.

[37] N.R. Paliwal, A.K. Mungray, Ultrasound assisted alkaline hydrolysis of poly (ethylene terephthalate) in presence of phase transfer catalyst, Polym. Degrad. Stab. 98 (2013) 2094–2101, https://doi.org/10.1016/j.polymdegradstab.2013.06.030.

[38] M. Parravicini, M. Crippa, M.V. Bertele', Method and apparatus for the recycling of polymeric materials via depolymerization process, WO 2013/014650 A1, January 31, 2013. ⟨https://patents.google.com/patent/WO2013014650A1/en⟩.

[39] Carbios. ⟨https://www.carbios.com/en/carbios-annonce-le-demarrage-de-son-demonstrateur-industriel-exploitant-sa-technologie-unique-de-recyclage-enzymatique-c-zyme/⟩, (accessed 15 February 2022).

[40] F.G. Barla, T. Showalter, H. Cheng Su, J. Jones, I. Bobe,. Methods for recycling cotton and polyester fibers form waste textiles, US 10,501,599 B2, December 10, 2019. ⟨https://patents.google.com/patent/US10501599B2/en⟩.

[41] Eunomia, Zero Waste Europe, How circular is PET?. (2022). ⟨https://zerowasteeurope.eu/library/how-circular-is-pet/⟩, (accessed 3 February 2022).

[42] M. De Smet, M. Linder, A circular economy for plastics – Insights from research and innovation to inform policy and funding decisions, (2019). ⟨https://op.europa.eu/en/publication-detail/-/publication/33251cf9–3b0b-11e9–8d04–01aa75ed71a1/language-en/format-PDF/source-87705298⟩, (accessed 12 February 2022).

[43] J. Payne, P. McKeown, M.D. Jones, A circular economy approach to plastic waste, Polym. Degrad. Stab. 165 (2019) 170–181, https://doi.org/10.1016/j.polymdegradstab.2019.05.014.

[44] S. Huysveld, K. Ragaert, R. Demets, T.T. Nhu, D. Civancik-uslu, M. Kusenberg, Technical and market substitutability of recycled materials: Calculating the environmental benefits of mechanical and chemical recycling of plastic packaging waste, Waste Manag 152 (2022) 69–79, https://doi.org/10.1016/j.wasman.2022.08.006.

[45] G.P. Karayannidis, A.P. Chatziavgoustis, D.S. Achilias, Poly(ethylene terephthalate) recycling and recovery of pure terephthalic acid by alkaline hydrolysis, Adv. Polym. Technol. 21 (2002) 250–259, https://doi.org/10.1002/adv.10029.

[46] J. Fabia, A. Gawłowski, T. Graczyk, C. Ślusarczyk, Changes of crystalline structure of poly(ethylene terephthalate) fibers in flame retardant finishing process, Polim. /Polym. 59 (2014) 557–561, https://doi.org/10.14314/polimery.2014.557.

[47] H.L. Lee, C.W. Chiu, T. Lee, Engineering terephthalic acid product from recycling of PET bottles waste for downstream operations, Chem. Eng. J. Adv. 15 (2021), 100079, https://doi.org/10.1016/j.ceja.2020.100079.

[48] K. Matuszek, E. Pankalla, A. Grymel, P. Latos, A. Chrobok, Studies on the solubility of terephthalic acid in ionic liquids, Molecules 25 (2019) 80, https://doi.org/10.3390/molecules25010080.

[49] T. Phuong, T. Pham, C. Cho, Y. Yun, Environmental fate and toxicity of ionic liquids: A review, Water Res 44 (2010) 352–372, https://doi.org/10.1016/j.watres.2009.09.030.

[50] R. Huang, Q. Zhang, H. Yao, X. Lu, Q. Zhou, D. Yan, Ion-exchange resins for efficient removal of colorants in bis(hydroxyethyl) terephthalate, ACS Omega 6 (2021) 12351–12360, https://doi.org/10.1021/acsomega.1c01477.

[51] Y. Peng, J. Yang, C. Deng, Y. Fu, J. Deng, Acetolysis of waste PET for upcycling and life-cycle assessment study, (2022). Available at Research Square. https://doi.org/10.21203/rs.3.rs-1275958/v1.

[52] F. Alvarado Chacon, M.T. Brouwer, E.U. Thoden van Velzen, Effect of recycled content and rPET quality on the properties of PET bottles, part I: Optical and

mechanical properties, Packag. Technol. Sci. 33 (2020) 347–357, https://doi.org/10.1002/pts.2490.
[53] Y. Li, H. Yi, M. Li, M. Ge, D. Yao, Synchronous degradation and decolorization of colored poly(ethylene terephthalate) fabrics for the synthesis of high purity terephthalic acid, J. Clean. Prod. 366 (2022), 132985, https://doi.org/10.1016/j.jclepro.2022.132985.
[54] G. Viscusi, E. Lamberti, F. D'Amico, T. Loredana, G. Vigliotta, G. Gorrasi, Design and characterization of polyurethane based electrospun systems 2 modified with transition metals oxides for protective clothing applications, Soc. Sci. Res. Netw. 11 (2020) 1092–1099, https://doi.org/10.2139/ssrn.4267872.
[55] S. Kumar, C. Guria, Alkaline hydrolysis of waste poly(ethylene terephthalate): A modified shrinking core model, J. Macromol. Sci. - Pure Appl. Chem. 42 A (2005) 237–251, https://doi.org/10.1081/MA-200050346.
[56] J.R. González-Velasco, J.A. González-Marcos, M.P. González-Marcos, J.I. Gutiérrez-Ortiz, M.A. Gutiérrez-Ortiz, Cinética Química aplicada, Editorial Síntesis, 1999.
[57] S. Mishra, A.S. Goje, Chemical recycling, kinetics, and thermodynamics of alkaline depolymerization of waste poly(ethylene terephthalate) (PET), Polym. React. Eng. 11 (2003) 963–987, https://doi.org/10.1081/PRE-120026382.
[58] ASTM D5991–15, Standard Practice for Separation and Identification of Poly (Vynyl Chloride) (PVC) Contamination in Poly(Ethylene Terephthalate) (PET) Flake, 2018. https://doi.org/10.1520/D5991–15.
[59] A.P. Dos Santos Pereira, M.H.P. Da Silva, É.P. Lima, A. Dos Santos Paula, F. J. Tommasini, Processing and characterization of PET composites reinforced with geopolymer concrete waste, Mater. Res. 20 (2017) 411–420, https://doi.org/10.1590/1980-5373-MR-2017-0734.
[60] S. Zhang, A.R. Horrocks, A review of flame retardant polypropylene fibres, Prog. Polym. Sci. 28 (2003) 1517–1538, https://doi.org/10.1016/j.progpolymsci.2003.09.001.
[61] W. Gao, X. Ma, Y. Liu, Z. Wang, Y. Zhu, Effect of calcium carbonate on PET physical properties and thermal stability, Powder Technol. 244 (2013) 45–51, https://doi.org/10.1016/j.powtec.2013.04.008.
[62] R.M.R. Wellen, Effect of polystyrene on poly(Ethylene Terephthalate) crystallization, Mater. Res. 17 (2014) 1620–1627, https://doi.org/10.1590/1516-1439.302614.
[63] B. Demirel, A. Yaraş, H. Elçiçek, Crystallization behavior of PET materials, BAÜ Fen. Bil. Enst. Derg. Cilt. 13 (2011) 26–35.
[64] D. Mileva, D. Tranchida, M. Gahleitner, Designing polymer crystallinity: An industrial perspective, Polym. Cryst. 1 (2018) 1–16, https://doi.org/10.1002/pcr2.10009.
[65] C. hao Sun, X. ping Chen, Q. Zhuo, T. Zhou, Recycling and depolymerization of waste polyethylene terephthalate bottles by alcohol alkali hydrolysis, J. Cent. South Univ. 25 (2018) 543–549, https://doi.org/10.1007/s11771-018-3759-y.
[66] S. Mishra, V.S. Zope, A.S. Goje, Kinetic and thermodynamic studies of depolymerisation of poly(ethylene terephthalate) by saponification reaction, Polym. Int. 51 (2002) 1310–1315, https://doi.org/10.1002/pi.873.
[67] S. Singh, S. Sharma, A. Umar, S.K. Mehta, M.S. Bhatti, S.K. Kansal, Recycling of waste poly(ethylene terephthalate) bottles by alkaline hydrolysis and recovery of pure nanospindle-shaped terephthalic acid, J. Nanosci. Nanotechnol. 18 (2018) 5804–5809, https://doi.org/10.1166/jnn.2018.15363.
[68] T. Yoshioka, T. Motoki, A. Okuwaki, Kinetics of hydrolysis of poly(ethylene terephthalate) powder in sulfuric acid by a modified shrinking-core model, Ind. Eng. Chem. Res. 40 (2001) 75–79, https://doi.org/10.1021/ie000592u.
[69] T. Yoshioka, T. Motoki, A. Okuwaki, Kinetics of hydrolysis of PET powder in nitric acid by a modified shrinking-core model, Ind. Eng. Chem. Res. 40 (1998) 75–79, https://doi.org/10.1021/ie000592u.
[70] C.Y. Kao, B.Z. Wan, W.H. Cheng, Kinetics of hydrolytic depolymerization of melt poly(ethylene terephthalate), Ind. Eng. Chem. Res. 37 (1998) 1228–1234, https://doi.org/10.1021/ie970543q.
[71] A.S. Goje, S.A. Thakur, V.R. Diware, S.A. Patil, P.S. Dalwale, S. Mishra, Hydrolytic depolymerization of poly(ethylene terephthalate) waste at high temperature under autogenous pressure, Polym. Plast. Technol. Eng. 43 (2004) 1093–1113, https://doi.org/10.1081/PPT-200030031.
[72] R. López-Fonseca, I. Duque-Ingunza, B. de Rivas, L. Flores-Giraldo, J.I. Gutiérrez-Ortiz, Kinetics of catalytic glycolysis of PET wastes with sodium carbonate, Chem. Eng. J. 168 (2011) 312–320, https://doi.org/10.1016/j.cej.2011.01.031.